Proceedings of DETC:
Design Engineering Technical Conferences, 18-th Biennial Conference on Mechanical Vibration and Noise
Pittsburgh, Pennsylvania September 9-12, 2001

DETC2001/VIB-21571

DETERMINATION OF EXTERNAL FORCES -- APPLICATION TO THE CALIBRATION OF AN ELECTROMAGNETIC ACTUATOR

Izhak Bucher
Faculty of Mechanical Engineering, Technion,
Haifa 32000, ISRAEL
bucher@tx.technion.ac.il

Moshe Rozenstain
Faculty of Mechanical Engineering, Technion,
Haifa 32000, ISRAEL

ABSTRACT

A method for obtaining an accurate estimate of electromagnetic forces acting upon a vibrating structure is derived in this paper. The method was developed as a means for calibrating an electromagnetic excitation device where the electromagnetic force was sought to be estimated. The unique features of the proposed method are: (a) Compensation of inertial effects; (b) The method relies on indirect measurement of forces and displacements that are fed into an experimentally calibrated dynamical model. The calibration process allows us to precisely estimate distributed inertia and elastic forces and this allows us to model the relationship between the actually applied forces and various measurable physical parameters affected by the external forces. In the case of an electromagnetic device the affected parameters will be air- gap, current and magnetic flux. The lack of information in this case has lead us to a threefold approach where experimental data is combined with an analytical approach together with state- of-the- art measurement-techniques. The necessity to obtain an accurate account of the distribution of inertia in the structure necessitates a precise spatial model that was generated by means of a scanning laser- Doppler sensor. The analytical part involves the implicit estimation of Lagrange multipliers from an extended principal of virtual work.

INTRODUCTION

The indirect estimation of externally time-dependent forces applied to an elastic structure is treated in this paper. The presented method uses reaction forces, a few point wise displacement sensors and a previously obtained model to generate an estimate of external (electromagnetic) forces. The proposed approach was implemented for the calibration of an electromagnetic excitation device where some parametric model, preferably based upon magnetic circuit theory, was sought to be fitted. A precise estimate of the forces exerted by the electromagnetic device was compared with computed estimates that were based upon current and flux measurements.

Under moderately high frequencies, a significant source of error in the estimation of the external forces stems may arise from the neglected dynamics of the elastic structure on which the electromagnetic device was acting. When the dynamics of the vibrating structure or more specifically the inertia effects play a major role, the true external forces may deviate considerably from the ones computed from force-gauges data and static equilibrium. Distributed inertia and elastic effects share some of the load with the force gauges to an extent that a large deviation from an ideal case could occur.

In order to precisely compensate for the distributed inertia and elastic forces, a spatially dense measurement grid was employed with a scanning laser interferometer. The high spatial resolution combined with an extended principal of virtual work was used to find the functional relationship between the measured reaction forces, the external electromagnetic forces, the material and geometrical properties, and the spatially dense measured response.

The problem of estimating external forces from measured displacements is known to pose some difficulties falling under the category of 'inverse problems'. To remedy the problems associated with inverse problems a smooth model for the measured response and hence the inertia forces is used thus provided in effect some regularization and better conditioning.

The paper is structured as following: the general problem of indirectly estimating external forces is described in section 2. The proposed method of solution and the required measurement set-up is shown in section 3 and the experimental demonstration of the proposed method is introduced in section 4.

DEFINITION OF THE PROBLEM

The problem being solved can be explained with the aid of figure 1. An elastic structure is subject to time varying external loads $f_1(t),\dots f_m(t)$. The External forces cannot be directly measured thus several infinitely stiff force sensors measuring $R_1(t),\dots R_3(t)$ provide some information concerning the reaction forces. Also present are *NS* displacement sensors positioned at selected several locations. The proposed experimental system is schematically depicted in figure 1.

In order to obtain the equations of motion of the continuous structure, a discretization scheme is employed. Let the response of the structure, $\mathrm{u}(x,t)$, be decomposed as:

$$\mathrm{u}(x,t) = \sum_r \varphi_r(x) q_r(t) \qquad (1)$$

Where $\varphi_r(x)$ are space dependent basis functions and $q_r(t)$ are generalized time dependent co-ordinates.

Making use of Hamilton's extended principle (*L* and *V* are defined in Appendix A) we arrive at the familiar form:

$$\sum_r \left(\frac{d}{dt}\frac{\partial L}{\partial \dot{q}_r} - \frac{\partial L}{\partial q_r} \right)\delta q_r = \delta W\ , \qquad (2)$$

This form leads to the familiar Lagrange's equations [Baruh,1983,Geradin & Rixen, 1994].

The external forces, $f_1(t),\dots f_m(t)$ appear in the expression of the external (virtual) work, δW, but as the reactions are applied to infinitely stiff force gauges they do not perform any (virtual) work (holnomic constraints perform zero work, [Baruh, 1999, p.233]). This fact practically means that no information about the reactions is present in equation 2 in its current form. The sought external forces must therefore be estimated from the distributed stiffness and inertia forces that are not readily available.

Goal of this paper: The presented method strives to present and estimation method for externally applied forces by using experimentally obtained data, the geometric and material properties of the vibrating structure.

Method of solution

The information obtained from the infinitely stiff force gauges can be obtained from the Lagrange equations with a suitable formulation adapted to constrained systems ([Brauh,1999, pp. 260-262]). The method of constraint relaxation is being used to overcome the lack of information from the constrained force-gauges by combining the information provided by them with some estimate coming from previous modeling and displacement sensors.

In the method of the constraint relaxation, each constraint is being released at a time and the resulted motion indicated by new generalized coordinates, $a_n(t)$, $n = 1\dots NF$, along with the added virtual work are taken into account.

Figure 2 illustrates a possible virtual displacement the structure may undergo when one constraint is being released. When each constraint is released by an infinitesimal amount, a new expression for the displacement can be derived.

The expression for the total response can now take the form

$$\tilde{\mathrm{u}}(x,t) = \mathrm{u}(x,t) + \sum_n \psi_n(x) a_n(t)$$

$$\tilde{\mathrm{u}}(x,t) = \sum_r \varphi_r(x) q_r(t) + \sum_n \psi_n(x) a_n(t) \qquad (3)$$

Where $\psi_n(x)$ are rigid body motions related to the (constraint released) generalized coordinate - $a_n(t)$. It is assumed throughout this paper that the structure is supported on the rigid force-gauges in a statically determinate manner, this means that there will be 2 force gauges for the one dimensional bending problem presented in figure2.

With the revised new expressions for the kinetic - $\tilde{T}(q,a)$ and potential- $\tilde{V}(q,a)$ energies and the revised expression for the virtual work- $\delta\tilde{W}(\delta q, \delta a, f, R)$ (See Appendix) we are able to recast equation 2 for the constraint-relaxed generalized equations

$$\sum_r \left(\frac{d}{dt}\frac{\partial \tilde{L}}{\partial \dot{a}_r} - \frac{\partial \tilde{L}}{\partial a_r} \right)\delta a_r = \delta \tilde{W}\ , \qquad (4)$$

Where the equations of motion of the added DOFs, a_r are [Porat, 1990; Baruh, 1999]

$$\sum_r \left(\frac{d}{dt}\frac{\partial \tilde{L}}{\partial \dot{a}_r} - \frac{\partial \tilde{L}}{\partial a_r} \right)_{a_r=0} = \left.\frac{\partial\, \delta \tilde{W}}{\partial\, \delta a_r}\right|_{a_r=0}\ , \qquad (5)$$

Simplifying according to the extended expressions for kinetic, potential and external force that are provided in appendix A, we have (replacing without loss of generality the vector $\mathrm{u}(x,t)$ with a scalar $u(x,t)$, a similar assumption is being made for all the associated functions, $\psi_r(x), \phi_j(x)$)

$$\sum_j m_{rj}\ddot{q}_j(t) + k_{rj} q_j(t) = R_r(t) + \sum_n f_n(t)\psi_r(x_n) \qquad (6)$$

where

$$m_{rj} = \int_V \rho \psi_r(x)\phi_j(x) dV\ ,\ k_{rj} = \int_V [B(\psi_r(x))] \mathrm{C} \lfloor B(\phi_j(x)) \rfloor dV$$

and x_n is the spatial location where the n^{th} external force attacks the structure.

In the statically determinate case there is no strain energy associated with constraint relaxation, therefore, $k_{rk} = 0$. Re-writing equation (6) in matrix form

$$\begin{bmatrix} m_{11} & m_{12} & \cdots \\ m_{21} & m_{22} & \\ \vdots & & \ddots \end{bmatrix} \begin{pmatrix} \ddot{q}_1(t) \\ \ddot{q}_2(t) \\ \vdots \end{pmatrix} - \begin{pmatrix} R_1(t) \\ R_2(t) \\ \vdots \end{pmatrix} = \cdots$$
$$\begin{bmatrix} \psi_1(x_1) & \psi_1(x_2) & \cdots \\ \psi_2(x_1) & \ddots & \\ \vdots & & \end{bmatrix} \begin{pmatrix} f_1(t) \\ \vdots \\ f_N(t) \end{pmatrix} \qquad (7)$$

Equation (7) has a unique solution where several conditions are fulfilled:

<I> There are $N \le 6$ external forces

<II> The structure is supported by N force-gauges

<III> The removal of each force gauge gives rise to rigid body motion, $\psi_j(x)$

<IV> The $\psi_j(x)$, $j = 1 \ldots N$, are linearly independent

For example, in the case where N=2, we have:

$$\begin{pmatrix} f_1(t) \\ f_2(t) \end{pmatrix} = \cdots$$

$$\begin{bmatrix} \psi_1(x_1) & \psi_1(x_2) \\ \psi_2(x_1) & \psi_2(x_2) \end{bmatrix}^{-1} \left(\begin{bmatrix} m_{11} & m_{12} & \cdots \\ m_{21} & m_{22} & \cdots \end{bmatrix} \begin{pmatrix} \ddot{q}_1(t) \\ \ddot{q}_2(t) \\ \vdots \end{pmatrix} - \begin{pmatrix} R_1(t) \\ R_2(t) \end{pmatrix} \right) \quad (8)$$

Equation (8) provides the sought expression for the external forces. Assuming that the reaction forces $R_r(t)$ are measured we still lack inertia related terms, $\ddot{q}_1(t), \ddot{q}_2(t)$.. . The associated inertia terms need to be estimated and this is described below:

Estimating the inertia terms

As the purpose of this work to provide the basis for a real-time estimate of the external forces, the inertia terms must be estimated from a finite (in fact rather small) number of displacement sensors that are spread along the structure. The problem of estimating the inertia terms evolves into an equivalent problem where the generalized displacement terms are extracted from NS sensors, $s_1(t),.. s_{NS}(t)$. The NS sensors are combined with a previously obtained estimate having a very fine resolution that was obtained with the scanning laser.

The basis functions, $\phi_r(x)$, can be chosen to be the mode-shapes residing within the range of interest, or simply a numerical (black-box) representation consisting of a linearly independent selection of functions. The modal approach has the advantage of being based on a physical interpretation, but this approach may have the disadvantage of neglecting out-of-band modes including the static response. The black-box approach can be constructed from an orthonormal set of functions that could provide a superior numerical conditioning compared with the former method, especially when this combination is to be extracted from a laboratory experiment. In this work we chose the black-box approach that may seem to have some redundant terms from a physical modeling point of view, but numerically this proved to be a more accurate choice as is demonstrated in the experimental part.

The deflection surface at a single frequency (or curve in the one- and two-dimensional cases) is developed in a series of orthonormal functions of space, $\beta_r(x)$:

$$\phi(x,\omega) = \sum_r p_r(\omega)\beta_r(x) \quad (9)$$

where the $p_r(\omega)$ are fixed for a given frequency under certain stationarity (steady-state) assumptions.

The total response can be expressed by a (finite) summation of the form:

$$u(x,t) = \sum_n \sum_r p_{n,r}(\omega)\beta_r(x) q_n(t) \quad (10)$$

where $q_n(t)$ are the generalized co-ordinates

Equation 10 contains several unknown quantities that need to be estimated. The space dependent coefficients, $p_{n,r}(\omega)$, are assumed to be known from an off-line experiment. These spatial basis functions allow us to devise quickly an estimate that is more suitable for real-time applications where only a limited amount of point sensors, $s_1(t),.. s_{NS}(t)$ is being used, (see figure 1).

Estimating the spatial coefficients

The coefficients from equation 10 - $p_{n,r}(\omega)$ are estimated at a single frequency by a standard least-squares approach that exploits the orthonormal functions $\beta_r(x)$ as basis functions to achieve better numerical conditioning.

With the scanning laser sensor, an estimate of the form

$$u(x,t) = \sum_n \left(\mu_n^c(x)\cos n\omega t + \mu_n^s(x)\sin n\omega t \right) \quad (11)$$

can be obtained where the spacing along x is Δx (can be made very fine without any loading of the structure that takes place when an accelerometer is being used)

A normalized estimate of the spatial amplitude is obtained by referring to the input signal (current in our case) as a means for aligning the phase. The sinusoidal Input signal for a measurement at $x = k\,\Delta x$ is can be modeled by

$$I(t) = I_k^c \cos \omega t + I_k^s \sin \omega t \quad (12)$$

Owing to the extremely high spatial resolution obtained with a scanning laser sensor, a very fine estimate of the normalized response at the excitation frequency and its multiples is obtained by [Rozenstein, 1999]

$$H_n(k\,\Delta x, \omega) = \frac{\mu_n^c(k\,\Delta x) - j\mu_n^s(k\,\Delta x)}{I^c - jI^s} \quad (13)$$

Here $H_n(k\,\Delta x, \omega)$ is the complex amplitude of the n^{th} harmonic of ω at $x = k\,\Delta x$.

The real part of the normalized response can be expressed as

$$\Re\left[H_n(\Delta x, \omega) \quad H_n(2\Delta x, \omega) \quad \cdots \right] = \cdots$$

$$\left[p_{n,1}(\omega) \quad p_{n,2}(\omega) \quad \cdots \right] \begin{bmatrix} \beta_1(\Delta x) & \beta_1(2\Delta x) & \cdots \\ \beta_2(\Delta x) & \beta_2(2\Delta x) & \\ \vdots & & \end{bmatrix} \quad (14)$$

Where $\Re$ symbolizes the real part of an element and a similar procedure can be applied to the imaginary part.

Equation 14 can be solved in the least-squares sense to provide the sought coefficients $p_{n,1}(\omega), p_{n,2}(\omega)$ ..

Estimating the generalized coordinates

Once the spatial basis functions have been estimated, we are able to provide a quick estimate of the generalized coordinates. Several sensors, $s_1(t),.. s_{NS}(t)$, are deployed along the structure at the spatial locations $x = l_1,.. l_{NS}$ respectively. For each sensor we are able to use equation 9 and write

$$s_j(t) = w(l_j, t) = \sum_n q_n(t) \sum_r p_{n,r}\, \beta_r(l_j) \stackrel{\Delta}{=} \sum_n q_n(t) \gamma_n(l_j) \quad (15)$$

where, $\gamma_n(l_j) = \sum_r p_{n,r}\, \beta_r(l_j)$. Re-writing equation 15 in matrix form, we have

$$\begin{pmatrix} s_1(t) \\ \vdots \\ s_{NS}(t) \end{pmatrix} = \begin{bmatrix} \gamma_1(l_1) & \gamma_2(l_1) & \cdots \\ \gamma_1(l_2) & \gamma_2(l_2) & \\ \vdots & & \end{bmatrix} \begin{pmatrix} q_1(t) \\ \vdots \\ q_{Nq}(t) \end{pmatrix} \quad (16)$$

from which, a unique solution for the generalized coordinates can be obtained (in the least-squares sense) under the restriction that $Nq \leq N$ (and the linear independence of the basis functions).

The proposed method is best illustrated with an example taken from a real experiment.

THE EXPERIMENTAL SYSTEM - AN EXAMPLE

An experimental system was set-up which consisted of a flexible steel beam mounted on 2 force-gauges by a knife-edge tip. The system was subject to external electo-magnetic force as described in figures 2, 4 and 5. The main purpose of this system is to provide a calibration means for the elecro-magnetic excitation device. In addition to the mechanical quantities, i.e. force, displacements some electrical quantities e.g. current, magnetic-flux were measured in parallel. These measurements allowed us to compare estimates of the electro-magnetic forces obtained independently from the proposed algorithm and some basic electrical engineering –based expressions.

For the frequency range of interest, the system was modeled as undergoing one-dimensional bending vibrations. Figure 4 shows a schematic layout of the various components and their *x*-axis location. In particular the co-ordinate locations of the force-gauges, point-sensors and electro-magnetic actuator are shown. The coefficients that are required in equation 7 are first estimated and the necessary estimates for the generalized co-ordinates leading to the inertia terms follow.

4.1 Estimating the basis displacement-functions

Inspecting figures 2 and 5 we are able to formulate the rigid body motions related to the releasing of the constraints, $a_1(t), a_2(t)$:

$$\psi_1(x) = \left(1 - \frac{x}{L}\right) \quad ; \quad \psi_2(x) = \left(\frac{x}{L}\right) \quad (17)$$

It was decided to consider the range 0 to 200 Hz and in this range it was found (see figure 3 below) that there is a single basis function $\phi_1(x)$. In this case the external electromagnetic is a non-linear function of the displacement. Indeed the force behaves according to [Schweitzer, 1994]

$$f = K \frac{i^2}{s^2} \quad (18)$$

Where *K* is a constant, *i* – current in the coils, *s* – air gap.

K is a function of the area of the poles – *A,* the number of turns – *N,* the permeability - μ, μ_0

Performing the measurement procedure as described above figure 3 was obtained.

It was found that under pure-tone sinusoidal voltage the elastic response is proportional to a single basis function. In this case equation 3 simplifies into

$$\tilde{u}(x,t) = \phi_1(x) \sum_n q_n(t) + \left(1 - \frac{x}{L}\right) a_1(t) + \left(\frac{x}{L}\right) a_2(t) \quad (19)$$

Estimating the generalized co-ordinates

Due to the nonlinear nature of equation 18 (as was measured in practice, see figure 7), we have

$$\sum_n q_n(t) = \sum_n \left(\sigma_n^c \cos n\omega t + \sigma_n^s \sin n\omega t\right) \quad (20)$$

The deflection is measured by two proximity-probe sensors , $s_1(t)$, $s_2(t)$ and therefore from equation 16 and the abovementioned simplifications we have

$$\begin{pmatrix} s_1(t) \\ s_2(t) \end{pmatrix} = \begin{bmatrix} \phi_1(l_1) \\ \phi_1(l_2) \end{bmatrix} \sum_n q_n(t) \quad (21)$$

A straightforward least-squares solution, assuming identical noise-variance for the two sensors, would be

$$\sum_n q_n(t) = \begin{bmatrix} \phi_1(l_1) \\ \phi_1(l_2) \end{bmatrix}^{\#} \begin{pmatrix} s_1(t) \\ s_2(t) \end{pmatrix} = \frac{\phi_1(l_1) s_1(t) + \phi_1(l_2) s_2(t)}{\phi_1^2(l_1) + \phi_2^2(l_1)} \quad (22)$$

Here # symbolizes a generalized inverse (having a closed form expression for this case)

It is thus possible to curve-fit the coefficients of the Fourier series as indicated by equation 20 extract the estimate in equation 22. Both equation 22 and the extraction of the Fourier terms can be realized by real-time (recursive) algorithms, but the presentation of such a formulation is beyond the scope of this paper (the reader is referred to Ljung, 1987 for further details on recursive estimation).

Estimating the inertia terms

Having identified the Fourier coefficients in equation 20, the acceleration can be directly computed by

$$\frac{d^2}{dt^2} \sum_n q_n(t) = -\sum_n (n\omega)^2 \left(\sigma_n^c \cos n\omega t + \sigma_n^s \sin n\omega t\right) \quad (23)$$

thus providing a larger weight to higher harmonics. Indeed figures 7,8 show some real data where the higher harmonics are evidently amplified. It can be seen in figure 8 that the inertia term contributes about 18% of the total magnitude and therefore is by no means negligible.

Using equation 8, the external forces we can now express the external forces in a closed form expression, where for this example, we have

$$\begin{pmatrix} f_1(t) \\ f_2(t) \end{pmatrix} = L\begin{bmatrix} L-L_2 & L-L_3 \\ L_2 & L_3 \end{bmatrix}^{-1} \begin{pmatrix} \ddot{q}_1(t)\int_0^L \rho A\left(\frac{L-x}{L}\right)\phi_1(x)dx \\ \ddot{q}_1(t)\int_0^L \rho A\left(\frac{x}{L}\right)\phi_1(x)dx \end{pmatrix} - \begin{pmatrix} R_1(t) \\ R_2(t) \end{pmatrix} \qquad (24)$$

Equation 24 was used to estimate the electromagnetic forces under various parameter changes. As an example figure 8 that compares the estimated force with and without the inertia term is shown. It can be seen that this term has a significant contribution to the total forces and cannot be neglected. The method that was shown here allowed us to estimate the electromagnetic force under various operating conditions that included the air-gap, DC and AC currents as shown in figure 9. Several calibration formulae were developed with this apparatus using the proposed algorithms but this part is beyond the scope of this paper.

CONCLUSION

This work develops a method that combines an analytical model with experimentally obtained one to estimate external forces given the reaction-forces and some displacement measurements. The use of a scanning laser sensor together with an extended Hamilton's principle provided closed form estimates for the, usually neglected inertia and elastic forces acting on a vibrating structure. It was shown in this paper that a carefully designed experiment with several forces-gauges will give rise to a structure that is statically determinate and thus only inertia correction terms need to be added to reconstruct the sought external forces. Inertia forces can be accurately estimated from the distribution of mass and estimation displacements in time, contrary to elastic forces that are much more difficult to estimate. An experimental rig was used to illustrate the usefulness of the proposed method and indeed this device was used to calibrate an electromagnetic actuator with good accuracy. The comparison of the estimated forces with quantities based on air-gap, current or flux measurements allowed us to develop some working formulae for the electromagnetic force. This part is reported elsewhere.

ACKNOWLEDGMENTS

The support of the Israeli Science Foundation is gratefully acknowledged

REFERENCES

1. Porat Y. , 1990, *Analytical Dynamics - lecture notes*, Technion, ISRAEL
2. Baruh H. 1999, Analytical Dynamics, McGraw-Hill
3. Geradin M. and RIXEN D.,1994, Mechanical Vibrations: Theory and application to structural dynamics, Wiley
4. Roezenstein M., 1999, "Determination of Magnetic forces", Master thesis, Technion
5. Schweitzer G. et al 1994, *Active Magnetic Bearings, ETH*
6. Ljung L. & Sodestrum, 1987, Theory and practice of recursive identification, Prentice-hall

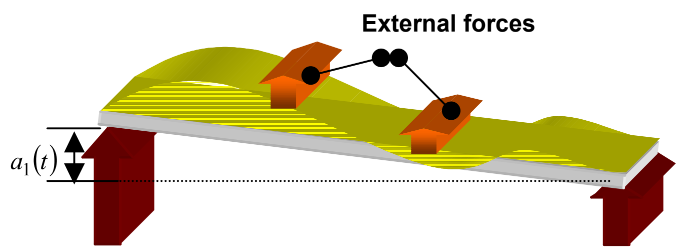

Figure 1: Two-dimensional structure showing the reactions and the external forces applied by an electromagnetic device

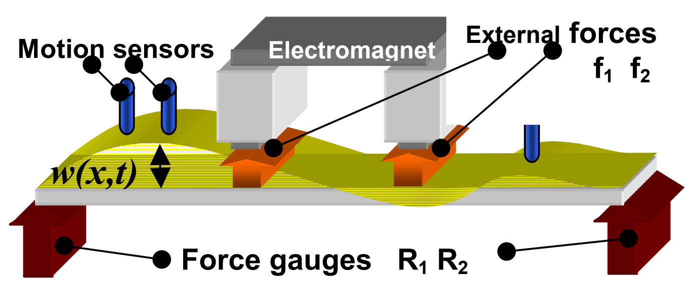

Figure 2: Two-dimensional structure undergoing a virtual (rigid body) displacement due to relaxation of the constraint reaction force

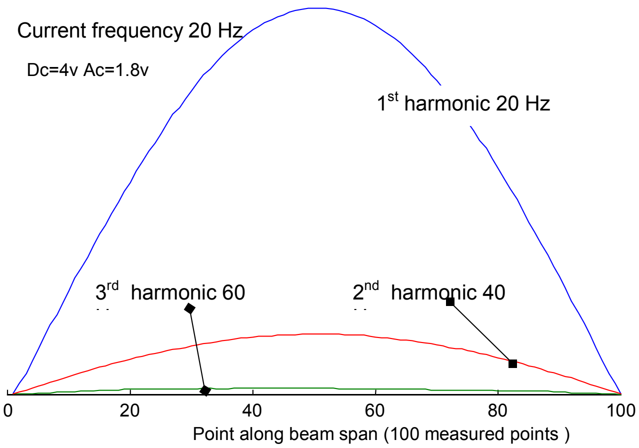

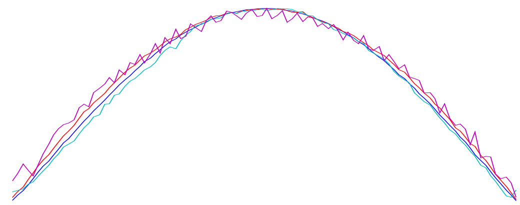

5 normalized amplitude distributions at of harmonics at 20, 40, 60, 80, 100 Hz Measured with scanning laser sensor

Figure 3. **Left**: Measured distribution of the first 3 harmonics of beam's deflection.
Right: normalized amplitude of the first 4 harmonics, showing a nearly identical amplitude distribution.

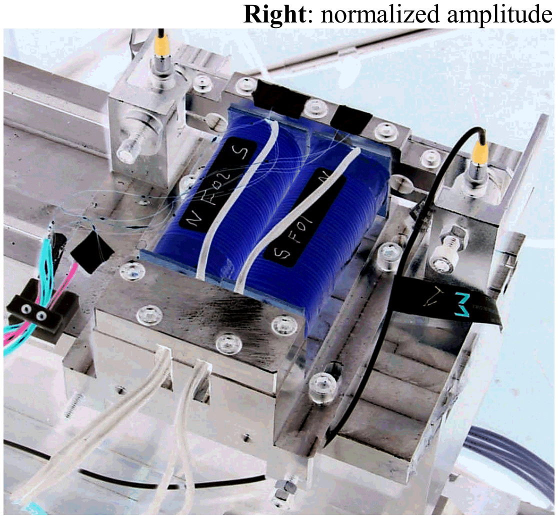

Figure 4. Photograph of the experimental rig

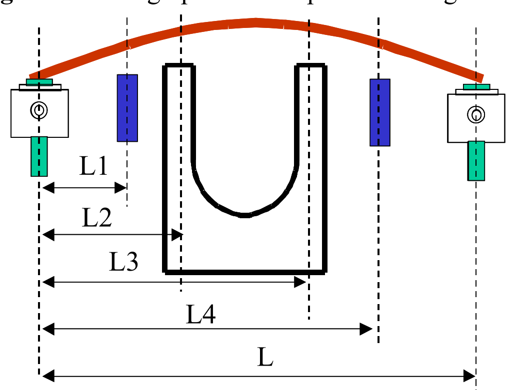

Figure 5 Locations of the force gauges, sensors (s_1 s_2 at L_1, L_4), magnetic forces (F_1 F_2 at L_2, L_3), and the reactions at force-gauges - R_1 R_2 (acting at both ends of the beam).

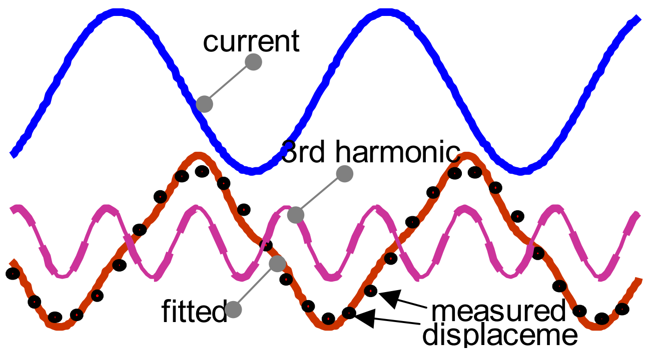

Figure 6. Time histories of the measured current and displacements Vs. the fitted Fourier

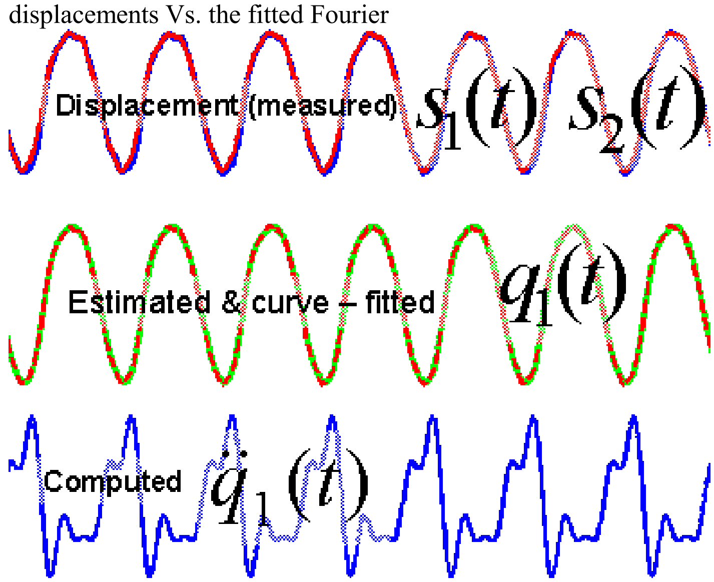

Figure 7. Time histories of the measured displacements (top), the computed and fitted generalized coordinate (middle) and the computed acceleration according to eq. 20 (bottom), (plots are not to scale)

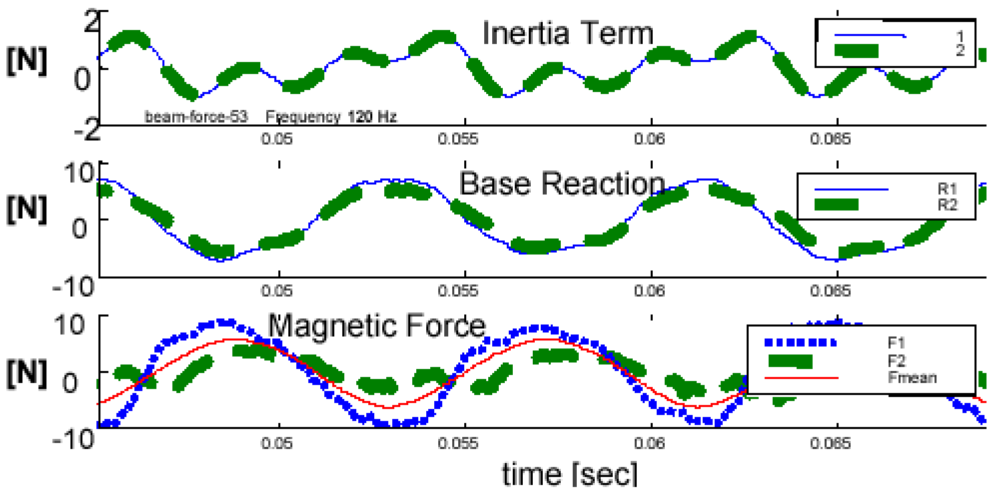

Figure 8. **Top**: The estimated contribution of the inertia force. **Middle**: Measured reaction-forces. **Bottom**: Reconstructed magnetic forces, left, right and mean

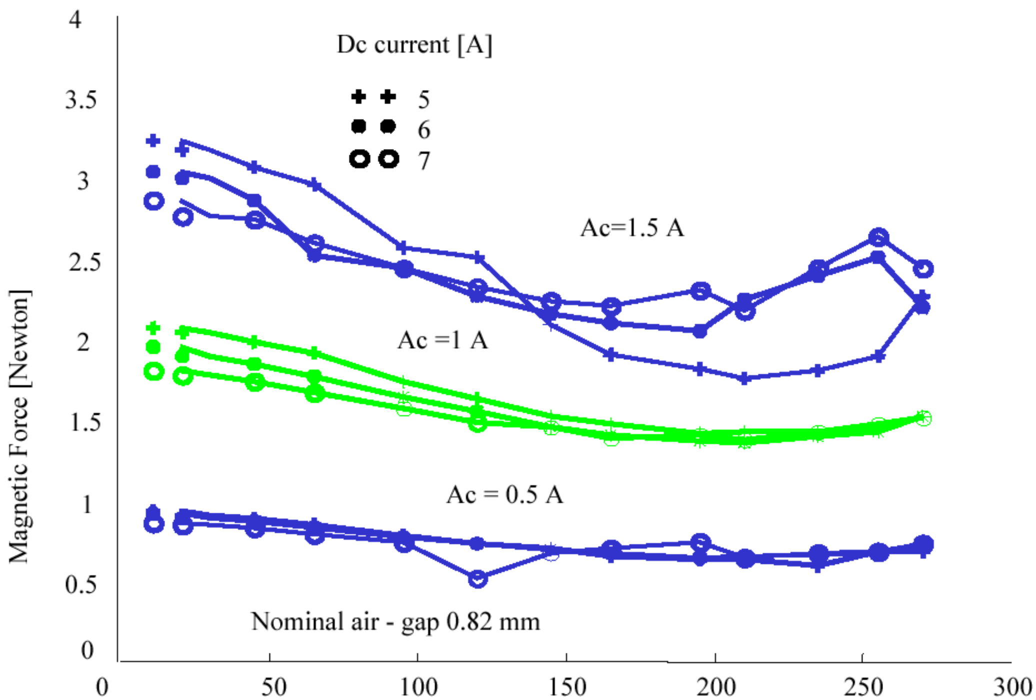

Figure 9. Reconstructed mean magnetic force as a function of the DC and AC current.
Several experiment were conducted to demonstrate the repeatability of the estimation method

Appendix A

The Largrangian is defined as $L = T - V$ where T is the kinetic energy while V represents the potential energy. Additionally, W - represents the external work performed by non-conservative forces (BARUH, 1999).

The kinetic energy can be computed by integrating over the domain Ω.

$$T = \frac{1}{2}\iint_{\Omega} \rho \dot{\mathrm{u}}(\mathrm{x},t)\cdot\dot{\mathrm{u}}(\mathrm{x},t)d\Omega \qquad \text{(A1)}$$

Similarly, the potential energy

$$V = \frac{1}{2}\iint_{\Omega} [\mathrm{B}(\mathrm{u})]^T \mathrm{C}[\mathrm{B}(\mathrm{u})]d\Omega \qquad \text{(A2)}$$

where $\mathrm{B}(\cdot)$ is a differential operator representing strain and **C** is a matrix containing material constants [Geradin, 1994].

Making use of equations 3, A1 and A2, we obtain:

$$\tilde{T} = \frac{1}{2}\int_{\Omega}\rho\left(\frac{\partial\tilde{u}(x,t)}{\partial t}\right)^2 dV = \frac{1}{2}\int_{\Omega}\left(\sum_r\sum_k \phi_r(x)\phi_k(x)\dot{q}_r(t)\dot{q}_k(t) + \cdots\right.$$
$$\left. + \sum_r\sum_k \psi_r(x)\psi_k(x)\dot{a}_r(t)\dot{a}_k(t) + \sum_r\sum_k \psi_r(x)\phi_k(x)\dot{a}_r(t)\dot{q}_k(t)\right)d\Omega \qquad \text{(A3)}$$

$$\tilde{V} = \frac{1}{2}\int_{\Omega}[B(\tilde{u}(x,t))]^T \mathrm{C}B[B(\tilde{u}(x,t))]d\Omega \qquad \text{(A4)}$$

$$\tilde{V} = \frac{1}{2}\int_{\Omega}\sum_r\sum_n q_r(t)q_n(t)[B(\phi_r(x))]^T \mathrm{C}[B(\phi_n(x))] +$$
$$+ \sum_r\sum_n a_r(t)a_n(t)[B(\psi_r(x))]^T \mathrm{C}[B(\psi_n(x))] + \ldots \qquad \text{(A5)}$$
$$+ \sum_r\sum_n q_r(t)a_n(t)[B(\phi_r(x))]^T \mathrm{C}[B(\psi_n(x))]d\Omega$$

Finally the virtual work performed by a virtual movement of the force-gauges can be expressed as:

$$\delta\tilde{W}(x,t) = \sum_r R_r \delta a_r(t) + \sum_n f_n(t)\,\delta\tilde{u}(x_n,t) \qquad \text{(A6)}$$

Now, the virtual displacement is

$$\delta\tilde{\mathrm{u}}(x,t) = \sum_r \varphi_r(x)\delta q_r(t) + \sum_n \psi_n(x)\delta a_n(t) \qquad \text{(A7)}$$

Hence the virtual work due to a virtual displacement of the constraints, becomes

$$\delta\tilde{W}(x,t) = \sum_r R_r \delta a_r(t) + \sum_n f_n(t)\sum_r \psi_r(x_n)\delta a_r(t) \qquad \text{(A8)}$$

$$\delta\tilde{W}(x,t) = \left(\sum_r R_r + \sum_r\sum_n f_n(t)\,\psi_r(x_n)\right)\delta a_r(t) \qquad \text{(A8)}$$

Thus the p^{th} generalized force can be identified as

$$Q_p = \frac{\partial\delta\tilde{W}(x,t)}{\partial\delta a_p(t)} = R_p + \sum_n f_n(t)\,\psi_p(x_n) \qquad \text{(A9)}$$

The inertia terms can be obtained from equations A3 and 5, and the only non-zero terms that are obtained from

$$\tilde{T} = \left.\frac{\partial\tilde{T}}{\partial\dot{a}_p}\right|_{a_r=0,\forall r} \qquad \text{(A10)}$$

By inspection of equation A3, we see that equation A10 becomes

$$\left.\frac{\partial\tilde{T}}{\partial\dot{a}_p}\right|_{a_r=0,\forall r} = \frac{1}{2}\int_{\Omega}\left(\sum_r\sum_k \psi_r(x)\phi_k(x)\dot{q}_k(t)\right)d\Omega \qquad \text{(A11)}$$

Further derivation with respect to time (As required by Largange's equations yields (After re-arranging terms)

$$\frac{d}{\partial t}\left.\frac{\partial\tilde{T}}{\partial\dot{a}_p}\right|_{a_r=0,\forall r} = \left[\frac{1}{2}\int_{\Omega}\left(\sum_r\sum_k \psi_r(x)\phi_k(x)\right)d\Omega\right]\ddot{q}_k(t) \qquad \text{(A12)}$$

The expression in brackets is constant and in the text we use

$$m_{rk} = \left[\frac{1}{2}\int_{\Omega}\left(\sum_r\sum_k \psi_r(x)\phi_k(x)\right)d\Omega\right] \qquad \text{(A13)}$$

A good design of the calibration system would yield $B(\phi_n(x)) = 0$, therefore the contribution of deformation energy to the measured forces disappears. For sake of generality the effect of deformation energy can be obtained in a similar manner and the result is provided in equation 6.